Static stability predicts the continuum of interleg coordination patterns in *Drosophila*

Nicholas S. Szczecinski[1,2,+], Till Bockemühl[1,+,*], Alexander S. Chockley[1], and Ansgar Büschges[1]

Affiliations:

[1] Department of Animal Physiology, Zoological Institute, University of Cologne, 50674 Cologne, Germany

[2] Present address: Case Western Reserve University, Department of Mechanical and Aerospace Engineering, USA

[+] Shared first authors, both authors contributed equally

[*]Author for correspondence (till.bockemuehl@uni-koeln.de)

Keywords:

motor control, locomotion, insect walking, stability, interleg coordination

Summary statement:

A simple stability-based modelling approach can explain why walking insects use different leg coordination patterns in a speed-dependent way.

Abstract

During walking, insects must coordinate the movements of their six legs for efficient locomotion. This interleg coordination is speed-dependent; fast walking in insects is associated with tripod coordination patterns, while slow walking is associated with more variable, tetrapod-like patterns. To date, however, there has been no comprehensive explanation as to why these speed-dependent shifts in interleg coordination should occur in insects. Tripod coordination would be sufficient at low walking speeds. The fact that insects use a different interleg coordination pattern at lower speeds suggests that it is more optimal or advantageous at these speeds. Furthermore, previous studies focused on discrete tripod and tetrapod coordination patterns. Experimental data, however, suggest that changes observed in interleg coordination are part of a speed-dependent spectrum. Here, we explore these issues in relation to static stability as an important aspect for interleg coordination in *Drosophila*. We created a model that uses basic experimentally measured parameters in fruit flies to find the interleg phase relationships that maximize stability for a given walking speed. The model predicted a continuum of interleg coordination patterns spanning the complete range of walking speeds as well as an anteriorly directed swing phase progression. Furthermore, for low walking speeds the model predicted tetrapod-like patterns to be most stable, while at high walking speeds tripod coordination emerged as most optimal. Finally, we validated the basic assumption of a continuum of interleg coordination patterns in a large set of experimental data from walking fruit flies and compared these data with the model-based predictions.

Introduction

Walking is an important behavior for most terrestrial animals; in many species, it is the primary mode of locomotion used in various contexts such as foraging, migrating, finding mates, hunting, or escape. Because of its importance for these behaviors, it can be assumed that walking has become highly optimized during evolution to enable the animal to reliably complete these tasks. However, walking is not a fixed behavior and must be adaptable regarding basic parameters like speed and direction. The most prominent of such adaptations is interleg coordination—the temporal and spatial relationships between leg movements. In large vertebrates like dogs, horses, and humans, changes in walking speed are accompanied by changes in interleg coordination, termed *gait* transitions (Alexander, 1989). A gait can be defined as a distinct mode of locomotion used within a particular speed range. For instance, a horse will first walk at low speeds, then transition to trot at an intermediate speed and, finally, switch to gallop at high speeds (Orlovsky et al., 1999). The transition between two gaits occurs at a characteristic locomotion speed and is discontinuous regarding at least one parameter (e.g., duty cycle of stepping or interleg phase relationships) associated with walking behavior (Alexander, 1989). It is important to note that gaits are not defined by a particular set of movement parameters but by a discontinuous, rather than gradual, transition between them. For the purpose of the present study, we will use this general definition by Alexander (1989) when we refer to gaits.

Interleg coordination during walking has also been studied extensively in arthropods, mainly in insects (for reviews see Ayali et al., 2015; Bidaye et al., 2017; Borgmann and Büschges, 2015; Cruse, 1990b; Schilling et al., 2013). As in vertebrates, these animals adapt their interleg coordination as they change walking speed (Graham, 1972; Wahl et al., 2015; Wendler, 1964; Wilson, 1966; Wosnitza et al., 2013). Several prototypical patterns have been described in the literature; insects use wave gait coordination at low walking speeds (Hughes, 1952), tetrapod coordination at intermediate speeds, and tripod coordination at high speeds (Strauss and Heisenberg, 1990; Wosnitza et al., 2013). Each of these locomotion modes corresponds to a particular interleg coordination pattern. During wave gait coordination, at most one leg executes a swing phase at any given time, while metachronal waves of protraction progress from the hind to the front leg on each side of the animal's body. In tetrapod coordination, at most two legs are in swing phase at a particular time. Finally, tripod coordination is characterized by concurrent swing phases of ipsilateral front and hind legs and the contralateral middle leg.

Commonly, these interleg coordination patterns in insects are referred to as gaits in the literature (Bender et al., 2011; Dürr et al., 2018; Nishii, 2000; Ramdya et al., 2017; Spirito and Mushrush, 1979); however, to our knowledge, it has never been explicitly shown that the

different forms of locomotion found in insects actually fulfill the definition of gaits as suggested by Alexander (1989)—namely, that these are discrete modes of locomotion and not merely special cases along a continuum. Knowing whether insects use discrete modes of locomotion as seen in vertebrates is important to understand the neural and biomechanical control strategies used by these animals and to compare and contrast with vertebrates. Discontinuous transitions from one mode of locomotion to the other would, for instance, imply the existence of at least two attractor states in the neuromechanical system responsible for locomotion. Such a multi-attractor system would probably require a very different structure compared to a single-attractor system.

Based on data from the cockroach *Periplaneta americana* (Hughes, 1952) and the stick insect *Carausius morosus* (Wendler, 1964), Wilson (1966) proposed a set of simple rules for the generation of interleg coordination in six-legged insects. In direct contrast to results from vertebrates (Alexander, 1989) and the common assumption of actual gaits in insects, these rules predicted that insects should use a speed-dependent continuum of stepping duty cycle and interleg phase angles. Wilson also pointed out that these rules should result in the natural emergence of all known interleg coordination patterns, including wave gait-like, tetrapod, and tripod coordination, as part of this continuum. Graham (1972) also supported this model with a detailed study of step timing in the stick insect *C. morosus*. Similarly, Spirito and Mushrush (1979) clearly showed a continuum of phase relationships between legs in walking *P. americana*. Results from *Drosophila melanogaster* support the notion of a continuum of coordination patterns; the tripod coordination strength calculated in a study by Wosnitza et al. (2013) showed no clear discontinuities when analyzed over the complete range of walking speeds.

These studies suggest that walking insects change interleg coordination in a speed-dependent, continuous, and systematic manner and either imply, describe, or explain this continuum. However, to our knowledge, there has been no explicit attempt to explain why these changes occur (i.e., what the adaptive value of these changes might be). Tripod coordination, which is typically used at high walking speeds, would also be suitable for slow walking; indeed, fruit flies can also use tripod coordination at lower speeds (Gowda et al., 2018; Wosnitza et al., 2013). However, the fact that a tendency for this shift can be observed in most insects suggests that some aspect of non-tripod interleg coordination patterns must be more optimal at lower speeds. Of course, exceptions are known: dung beetles (genus *Pachysoma*), for instance, sometimes use a peculiar galloping gait (Smolka et al., 2013), and *P. americana* can switch to quadrupedal and even bipedal running during high-speed escape (Full & Tu, 1990).

In the present study, we explored the question of why walking insects change interleg coordination in a speed-dependent manner. In large animals, energy optimality is typically assumed to be the crucial factor responsible for the emergence of true gaits (Hoyt & Taylor, 1981), although there is evidence that stability also plays a role in this (McGhee and Frank, 1968; Wilshin et al., 2017). Here, we consider static stability during walking as a potentially important parameter and hypothesize that it may play a role for interleg coordination in insects because they are typically small and their size makes their inertia less important or even negligible compared to the elastic forces of their muscles and joints or the viscous forces from the air around them (Hooper, 2012; Hooper et al., 2009). To investigate the influence of static stability on coordination, we devised a compact model that incorporates several kinematic parameters that are known from walking fruit flies (*D. melanogaster*), such as swing duration, stance amplitude, and stance trajectory. Fruit flies spontaneously walk at various speeds, so data from these animals is well suited to explore a large range of walking speeds (Mendes et al., 2013; Strauss and Heisenberg, 1990; Wosnitza et al., 2013). The model was used to exhaustively test all theoretically possible coordination patterns (defined herein as phase relationships between ipsilaterally or contralaterally adjacent legs) for all experimentally observed walking speeds in *D. melanogaster*. The predicted phase relationships between legs were then compared with a large body of corresponding data from walking flies.

The results herein suggest that static stability plays a role in the selection of interleg phase relationships. At high reference walking speeds, our model predicts that tripod-like coordination is the optimal coordination pattern for maintaining static stability. This preference for tripod-like coordination changes when the reference speed is lowered to speeds that, in the fruit fly, are found in the intermediate or slow range; here, the timing of the different legs' power strokes is less tightly correlated, and the animal takes advantage of more stable coordination patterns. The patterns predicted by the model resemble tetrapod-like and wave gait-like coordination. Importantly, the model predicts a continuum of coordination patterns that smoothly vary with walking speed. Experimental data confirm that walking flies shift their coordination in a similar way; their motor output seems to also reflect not only theoretically attainable stability but also how robustly such stability can be realized in the presence of locomotor variability.

Materials and Methods

Stability model

Based on previous experimental findings (Wosnitza et al., 2013) we created a model that incorporates several key aspects of walking in *D. melanogaster* and explicitly addresses the speed-dependent nature of interleg coordination. It should be noted that this model is also consistent with observations in the stick insect *C. morosus*, a perennial model of insect locomotion (Graham, 1972). The model makes the following assumptions:

1. The duration of stance, T_{st}, depends on walking speed, V_{body} (assuming no slip).
2. Each leg's stepping frequency, f_{step}, depends on walking speed.
3. The duration of swing phase, T_{sw}, does *not* depend on walking speed.
4. The stance amplitude, s, does *not* depend on walking speed.
5. The phase relationships between each pair of ipsilateral legs are identical, ϕ_I.
6. The phase relationships between each pair of contralateral legs are identical, ϕ_C.

These values can be related by a number of equations. The speed of the body is the speed of each foot while in stance phase,

$$V_{body} = {}^{s}/_{T_{st}}. \quad (1)$$

This equation can be rearranged to solve for T_{st}. The stepping frequency is the inverse of the stepping period, which has two components, the duration of the swing movement and the duration of stance movement,

$$f_{step} = \frac{1}{T_{sw}+T_{st}}. \quad (2)$$

The stepping frequency can be expressed as an explicit function of the body speed by rearranging Equation 1 and substituting it for T_{st} in Equation 2:

$$f_{step} = \frac{1}{T_{sw}+s/V_{body}}. \quad (3)$$

We also assume that the fly's locomotion has no airborne phase, thus constraining the duration of stance relative to the duration of swing:

$$T_{st} \geq T_{sw}. \quad (4)$$

Data from a previous study (Wosnitza et al., 2013) validate these assumptions and are presented in Figure 1. Least-squares fitting reveals that swing phase duration and step amplitude (as measured in the fly body's frame of reference) are only weakly correlated with

walking speed (Fig. 1A and B). In contrast, stance duration and step frequency are strongly correlated with walking speed. Importantly, both stepping frequency and stance duration can be accurately predicted assuming that swing duration and step amplitude are constant. Figure 1C plots Equation 1 over the experimental data using the leg-specific mean values for s and T_{sw} from Figure 1A and B. Figure 1D likewise plots Equation 3 over the experimental data. Both plots reveal that these equations strongly predict the experimental data, despite the fact that these are not least squares fits (green curves). In addition, Equation 4 places a theoretical upper limit on the model's speed (~15 BL s^{-1}). This upper limit also coincides with the maximal walking speed that is regularly observed in experimental data (Wosnitza et al., 2013).

The model presented here used these relations and a desired walking speed as a set point to calculate the corresponding stepping frequency and stance duration. Because our previous analysis showed that swing duration is very similar for all legs we used the global mean of all legs as swing duration (31 ms). The two parameters, stepping frequency and stance duration, were then used in conjunction with experimentally measured average stance trajectories (Fig. 2C; data from Wosnitza et al., 2013) to construct one complete step cycle for each leg. All stance trajectories were defined in relation to the center of mass (COM) of the fly. The COM's position was estimated by individual weight measurements of heads, thoraces, abdomina, sets of six legs, and the wings (n = 30). These measurements showed that the head contributed 12.5% of the fly's total weight, the thorax contributed 31%, and the abdomen 45%. The combined weight of the legs (11%) and the wings (0.5%) were neglected for the calculation of the center of mass. The head, thorax, and abdomen were then modeled as conjoined ellipses that had the same dimensions and relative positions as their counterparts. Using the individual weights and the positions and dimensions of the modeled body parts, we calculated the position of the COM.

During virtual swing movement, a leg's tarsus was lifted off at the posterior extreme position (PEP) and moved to the anterior extreme position (AEP). During the virtual stance movement, the tarsus touched down at the AEP and moved with a uniform speed (i.e., the set walking speed) to the PEP, where it was lifted off again. A virtual step in the model was defined as the time between two PEPs. For this interval, the instantaneous phase for each leg was linearly interpolated between 0 and 1, and two parameters, ϕ_I and ϕ_C, determined the phase relationships (equal to the phase difference) between the legs in this model (Fig. 2D); they, too, can adopt values between 0 and 1. ϕ_I defined ipsilateral phase relationships of step cycles between hind and middle legs and between middle and front legs. Each set of three ipsilateral legs was then treated as a unit (gray outline in Fig. 2D), and the phase relationship between these contralateral units was determined by ϕ_C. Thus, for a particular

walking speed and a set of phase relationships, a particular leg's position and whether it was in stance could be determined at a given time. The tarsal positions of the legs simultaneously in stance at a given time were used to determine a support polygon; the minimum distance between the COM and an edge of this polygon was defined as static stability (Fig. 2E). Static stability was positive when the COM was within the support polygon and 0 when it was outside. When there were fewer than three legs on the ground, static stability was undefined and set to 0.

We believe that the static stability is a good proxy for the total (i.e., dynamic) stability of the animal because of the fly's small size. First, the inertia of the limbs has a negligible effect on motion and control. This is because muscle stiffness scales with size to the 2nd power, but the moment of inertia of a limb segment scales with size to the 5th power. Thus, a fruit fly cannot use a momentum-based control strategy as a human would (Hooper et al., 2009). Second, fluid dynamics reveal that flies do not walk through the air as large animals do but rather wade through a viscous fluid. The Reynolds number measures the ratio between the inertial and viscous forces that a fluid applies to a solid object (Turns, 2006). The Reynolds number of a fly walking through air at its maximum observed walking speed, 30 mm s^{-1}, or approximately 15 body lengths (BL) s^{-1}, can be calculated to be about 4, corresponding to a very viscous, laminar regime (see also Table S1). Such motion would depend much more on static than dynamic stability. Thus, since the elastic and viscous forces acting on a fly would be much larger than the inertial forces, we conclude that the static stability should be a good proxy for the total stability of the animal.

For a set walking speed, a stepping frequency and stance duration were uniquely defined, and the average stance trajectories were assumed to be constant. Consequently, there were two adjustable parameters in this model: ϕ_I and ϕ_C. To determine static stability for different sets of ϕ_I and ϕ_C, each of the two phases was varied systematically from 0 to 1 in steps of 0.02. For each possible combination of phase relationships, we simulated one complete step cycle and calculated its minimum static stability; the minimum static stability over one complete step cycle was then defined as the static stability for a particular set of ϕ_I and ϕ_C. For one set walking speed, all stability values were normalized to the maximum found for this speed. Thus, coordination patterns for which the COM always remained within the support polygon returned positive values. Those with larger values keep the COM towards the center of the polygon at all times, increasing the margin of static stability.

We will also refer to the robustness of a given interleg coordination pattern (ICP). In the context of this paper, robustness means the *maximum permitted variation in phase angles before the ICP is no longer statically stable*. Note that this does not refer to mechanical robustness to external forces. If an ICP is *not* robust, this means that a small error in the

timing of a foot's touch down may cause the ICP to become statically unstable. We compute the robustness of a given ICP, (ϕ_C^*, ϕ_I^*), as the shortest distance in the phase space (ϕ_C, ϕ_I) to any point where the static stability equals zero. If the ICP in question is not statically stable, then the robustness is also zero.

Flies and animal husbandry

Fruit flies (*D. melanogaster*) were raised at a temperature of 25 °C and 65% humidity on a 12-h/12-h light/dark cycle. They were raised on a medium based on a recipe by Backhaus et al. (1984). Experimental data were based on three different fly strains for the experiments described herein: the wild-type strains *Berlin* and *CantonS* (WT, data from this study and Wosnitza et al., 2013) and the mutant strain w^{1118} (data from Wosnitza et al., 2013). These mutant flies have been reported to walk more slowly than wild-type strains, but show no other apparent impairments (Wosnitza et al., 2013). Flies used during experiments were between three and eight days old. Fly data presented in the manuscript were either obtained during free-walking or tethered walking.

Free-walking assay

A schematic of the free-walking setup is shown in Figure 3A. It consisted of an inverted glass petri dish that we used as a transparent arena (diameter 80 mm) held by a circular frame with a cutout below the dish. The cutout provided an unobstructed bottom view of the arena. A surface mirror was placed below the arena at a 45° angle; this allowed for video recordings at approximately the same height as the setup. In conjunction with the mirror, we used an infrared (IR)-sensitive high-speed camera (VC-2MC-M340; Vieworks, Anyang, Republic of Korea) to capture a bottom view of a central rectangular area on the surface of the arena of approximately 30 x 36 mm, with a resolution of 1000 x 1200 pixels, 200-Hz frame rate, and a shutter time of 200 µs. Illumination was provided by a ring of IR light-emitting diodes (LEDs) arranged concentrically around the arena and emitting their light mainly parallel to the arena's surface. This resulted in a strong contrast between background and fly (see Fig. 3B). The LEDs' activity was synchronized to frame acquisition of the camera. To prevent escape, the arena was covered with a watch glass that established a dome-shaped enclosure, similar to an inverted FlyBowl (Simon & Dickinson, 2010). To keep flies on the horizontal petri dish, we covered the inside of the watch glass with SigmaCote (Sigma-Aldrich, St. Louis, MO). Prior to an experiment, a single fly was extracted with a suction tube from its vial and placed onto the arena, which was then immediately covered with the watch glass. Flies were allowed to explore the arena for approximately 15 minutes, after which video acquisition was started.

Flies were spontaneously active in the arena and frequently crossed the capture area. Video data of this area was continuously recorded into a frame buffer of five-to-ten-second durations. During an experiment, custom-written software functions evaluated the recorded frames online and determined if a fly was present and if it had produced a continuous walking track that was at least 10 BL in length. Once the fly had produced such a track and either stopped or left the capture area, the contents of the frame buffer were committed to storage as a trial for further evaluation. Video acquisition and online evaluation during acquisition were implemented in MATLAB (2016b; The MathWorks, Natick, MA).

Tethered-walking assay

A schematic of the tethered walking setup is shown in Figure 3C. It is a modified version of a setup described previously (Berendes et al., 2016; Seelig et al., 2010). The setup consisted of an air-supported polypropylene (PP) ball (diameter 6 mm) onto which a tethered fly can be placed. Flies placed atop the ball in this manner will show spontaneous walking behavior and use the ball as an omnidirectional treadmill. Ball movements were measured by two optical sensors (ADNS-9500; Broadcom, Inc., San Jose, CA) with an acquisition speed of 50 Hz. Each of these sensors provided information about 2D optic flow at the equator of the ball; combining these data allowed for the reconstruction of the ball's rotational movement around its three axes of rotation. Based on these movements, we reconstructed the fly's instantaneous speed and the curvature of the virtual track during walking. Concurrently, and synchronized to the acquisition of these data, we recorded high-speed video with a resolution of 1200 x 500 pixels from a top view (other parameters and camera model same as above references). Illumination was provided by an IR LED ring positioned around the camera's lens (96 LEDs) and focused onto the fly. Low-level control of the optical sensors and synchronization to the camera was implemented with custom-made hardware (Electronics Workshop, Zoological Institute, University of Cologne), while high-level control and video data acquisition were implemented in MATLAB. To improve visibility of the fly's legs, we placed two surface mirrors on a gantry above the fly. The surface of the mirrors formed an angle of 25° with the optical axis of the camera and, thus, provided two additional virtual camera views (see Fig. 3D). Annotation of leg kinematics was done in these side views.

Prior to tethered-walking experiments, flies were cold-anesthetized and transferred into a fly-sized groove in a cooled aluminum block (~4 °C), which held them in place for tethering. Using a dissecting microscope, we then glued a copper wire (diameter 150 µm) to the fly's thorax. For this, we used dental composite (Sinfony™; 3M ESPE AG, Seefeld, Germany) that was cured within a few seconds with a laser light source (wavelength 470 nm). The wire was inserted into a blade holder which, in turn, was attached to a 3D micromanipulator used for

exact positioning of the fly atop the ball. Similar to the free-walking condition, flies were given approximately 15 min to familiarize themselves with the ball and the setup, as well as to recover from anesthesia. Kinematic data from the ball and video data from the camera were captured into separate ring buffers. Flies were spontaneously active; here, however, trial acquisition was not triggered automatically by fly activity, as done in the free-walking assay, but manually.

Data annotation and analysis

Prior to data analysis, we pre-selected trials that were straight and whose walking speed varied only little. In general, this ensured comparability with results from the model, in which we only considered straight walking. Furthermore, because we specifically excluded trials with large walking speed variability, we reduced the influence of inertial effects the PP ball might have had on the walking behavior. The position of the fly throughout a trial in the free-walking paradigm was determined automatically. In brief, each video frame was converted into a binary image, in which the fly was detected as the largest area. This area was fitted with an ellipse; its major axis and centroid were defined as the fly's orientation and center, respectively. Walking speed and rotational velocity were calculated as changes of the center and rotation over time. In each trial, the times and positions of all AEPs and PEPs of each leg were determined manually. These positions were then transformed into a body-centered coordinate system based on the fly's center and orientation. In the tethered-walking assay, walking speed and rotational velocity were provided directly by the ball's motion sensors. All positional data (speed and distance) were normalized to BL and subsequent analyses were carried out on these body-centered and BL-normalized data.

An individual step was defined as the movement of a leg between two subsequent PEPs. Swing movement was defined as the movement between a PEP and the subsequent AEP; stance movement was defined as the movement between an AEP and the subsequent PEP. The walking speed associated with one step was defined as the average walking speed throughout the step. The instantaneous phase of a step was defined as a value between 0 and 1, which progressed linearly over time between the beginning and the end of the step. The phase relationship between a pair of legs was calculated based on the difference between the instantaneous phases of the two legs at the time of the PEP of one of the legs (i.e., the reference leg). All annotations and calculations were carried out with custom-written functions in MATLAB.

Results

Our model compactly represents possible interleg coordination patterns (ICP). Figure 4A shows a plot of the ipsilateral phase angle, ϕ_I, against the contralateral phase angle, ϕ_C, which we call a ϕvϕ plot. Each (ϕ_C, ϕ_I) ordered pair represents one ICP. Once a walking speed is set, the full stepping pattern can be determined based on the invariant features we introduced into our model. Figure 4B-E shows several exemplary ICPs corresponding to particular points in the ϕvϕ plot; walking speed was set to 5 BL s^{-1}. These examples are meant to give the reader an intuitive understanding of the ϕvϕ plot. For example, when ϕ_I is 1/3, tetrapod-like ICPs emerge (Figure 4B-D). Figure 4B and C illustrate ICPs that have been described in the literature as (ideal) tetrapod patterns, in which two legs always execute their swing movements at the same time; which legs swing together depends on ϕ_C (either 1/3 or 2/3). As we will show, these ideal tetrapod ICPs are not commonly observed in experimental data, where animals typically use ICPs like the one shown in Figure 4D. The ϕvϕ plot can also describe a tripod ICP (Figure 4E) commonly observed in fast-walking insects.

The ϕvϕ plots reveal which ICPs are predicted to be the most statically stable at each walking speed. Figure 5 shows the stabilities of all ICPs at various speeds (Fig. 5Ai-Hi) and the ICPs that correspond to the most stable values of ϕ_I and ϕ_C (Fig. 5 Aii-Hii). Generally, the area showing non-zero static stability decreases as walking speed increases. This trend indicates that, at low walking speeds, more combinations of ϕ_I and ϕ_C result in stable walking. However, unique maxima (i.e., optimal combinations of ϕ_I and ϕ_C) can be found for each walking speed. These phase values of highest static stability (red dots in Fig. 5Ai-Hi) indicate that, at low walking speeds, ϕ_I is approximately 0.2 (Fig. 5Ai) and increases continuously towards values of approximately 0.4 (Fig. 5Hi). ϕ_I will, in fact, converge to 0.5 at even higher walking speeds (data not shown). At the same time, the optimal value for ϕ_C remains 0.5 over the complete speed range. The footfall patterns associated with the optimal ϕ_I and ϕ_C values in Figure 5Aii-Hii resemble ICPs reported in the literature.

As walking speed increases, the stance phase duration becomes shorter, reducing the general size of the stable region in each plot. The model predicts that the variance of both ϕ_I and ϕ_C should decrease as walking speed increases, showing an increasingly smaller range of ϕ_I and ϕ_C during the transitions towards tripod. This decrease in variability has been described in the literature and is also apparent in the experimental data presented here (see Fig. 8).

The ϕvϕ plots also reveal which combinations of ϕ_I and ϕ_C are predicted to be the most robust to alterations of leg phasing at each walking speed. Figure 6 shows the robustness of all ICPs at various speeds. Even as the walking speed increases, the most robust values of

ϕ_I and ϕ_C do not vary. At every walking speed, tripod coordination, corresponding to ϕ_I = 0.5 and ϕ_C = 0.5, permits the largest fluctuations in ϕ_I and ϕ_C before the animal is no longer statically stable (red dots in Fig. 6A-H). Interestingly, the most stable ICPs predicted by the model are also not very robust (white dots in Fig. 6A-H). This suggests that the animal does not use the theoretically most stable ICP, but instead favors a different ICP that takes into account variability and does not require perfect timing to remain statically stable.

The most stable phase relationships predicted by the model have an anteriorly directed swing phase progression (SPP). This sequence, in which swing phase initiation progresses from the hind leg to the middle leg and ends in the front leg during a complete ipsilateral step cycle, has been described in many studies on six-legged walking in animals, both explicitly and implicitly. The model has not been tuned to adhere to this particular progression; it emerges naturally. Furthermore, as the static stability distribution suggests (Fig. 5Ai-Hi), a posteriorly directed sequence, corresponding to ϕ_I values between 0.5 and 1, would be noticeably less stable. This prediction implies a crucial role of the anteriorly directed SPP in walking.

Figure 7 explores the higher stability of the anteriorly directed SPP in more detail. To do this, we chose a very slow walking speed of approx. 2.5 BL s^{-1} (this corresponds to duty cycle of 5/6); at this speed, the model produces a wave gait-like ICP, and the effect of single legs lifting off can be examined. Figure 7A and 7B show the instantaneous stability for the model over the course of one complete step cycle. In both of these conditions, ϕ_C was set to 1/2. In Figure 7A, we set ϕ_I to 1/6 (anteriorly directed [AD] SPP); in Figure 7B, we set ϕ_I to 5/6 (posteriorly directed [PD] SPP). The static stability of the AD SPP has a higher minimum value, a higher average value, and less variation than the PD SPP, while the latter reaches a slightly higher maximum value. This can be explained by examining how the support polygon changes when a front or hind leg starts its swing movement. When a front leg enters swing, the change in static stability depends on where the middle leg is. When the SPP is AD (Fig. 7Ai and Aii), the static stability does not change appreciably because the ipsilateral middle leg has entered stance directly behind the front leg before it lifts off (Fig. 7C). This is in direct contrast to when the SPP is PD (Fig. 7Bi and Bii, and Fig. 7D), in which case the ipsilateral middle leg is farther posterior and about to enter swing itself. This results in the support polygon becoming drastically smaller when the front leg enters swing phase (red arrow, Fig. 7Bi). An analogous situation occurs when a hind leg enters swing, illustrated in Figures 7Aiii, 7Aiv, 7Biii, and 7Biv.

The most stable ICP predicted by the model always lies along the line ϕ_C = 0.5, and its value of ϕ_I depends continuously on the walking speed. To test the model's predictive ability with regard to these values, we analyzed a pooled dataset (collected in this study and Wosnitza

et al., 2013) of 9,552 steps (average of 1,592 steps per leg). For 4,372 contralateral comparisons and 5,849 ipsilateral comparisons ϕ_I and ϕ_C were well defined; in total, we analyzed 106 trials in 31 individuals. We limited our comparison with the model to steps that were produced at walking speeds between 3 and 10 BL s^{-1} during straight walking.

Figure 8 compares static stability-optimal values (magenta lines) with experimental data. Average contralateral phase relationships cluster around 0.5 (green lines, Fig. 8C-D) over the whole speed range, while average ipsilateral phase relationships increase smoothly from values of approximately 0.35 to 0.5 (green lines, Fig. 7A-B, 7F-G). The predicted contralateral phases are very similar to average experimental data (Fig. 7C-D, red and green lines). In addition, the experimental data's variability decreases towards higher walking speed, which might reflect the reduction in the range of values with non-zero static stability (see Fig. 5Ai to Hi). The predicted ipsilateral phases differ noticeably from average experimental data; predicted phase values for ϕ_I are lower than the experimental data. There is, however, a clear tendency towards lower phase values at lower walking speeds. Interestingly, the experimental data seem to be constrained by the optimal phase values predicted by the model at lower speeds, with almost no values below this lower boundary. Figure 6 indicated that the most stable ϕ_I are very close to values associated with low static stability or even static instability (white dots in Fig. 6), quantified by the plots of robustness. Intuitively, these values correspond to swing movement overlap in ipsilateral neighboring legs (i.e., between hind and middle, or middle and front leg, respectively); any perturbation in the ipsilateral phase relationship that shifts ϕ_I to this lower value will therefore drastically reduce static stability. As a consequence, the most stable ipsilateral phase is also the least robust; a small reduction in the ipsilateral phase would destabilize the animal's posture noticeably. Therefore, the animal appears to prefer more robust ICPs to the most stable ICP. This preference, in turn, is also evident in the contralateral phase angle data, in which the most stable ICP is also the most robust, and the animal behaves accordingly.

One should also note that the model does not predict the existence of the idealized tetrapod ICP, in which two predetermined legs simultaneously execute their swing movement. Instead, the model predicts a value of 0.5 for ϕ_C at all walking speeds. The resulting ICPs resemble a tetrapod pattern (i.e., at most two legs are in swing phase), but these legs do not enter swing phase simultaneously. The data in Figure 8 appear to support this, in that the experimental data's mean ϕ_C value is 0.5 at all speeds. It is possible, however, that this mean value arises from an underlying bimodal distribution with peaks at ϕ_C = 1/3 and ϕ_C = 2/3; these values would correspond to the two possible idealized tetrapod patterns described in the literature (see also Fig. 4B and C). In this case, animals would choose either of the two options with equal probability, resulting in an average value of 0.5. This, however, is not the

case (see Figure S1 and Supplementary Material); values of ϕ_C for slow-walking animals (< 5 BL s^{-1}) are normally distributed around 0.5. Our findings support the notion that fruit flies do not walk using the idealized tetrapod ICP but instead keep contralateral leg pairs in antiphase at all walking speeds. Finally, discrete gait changes, like those observed in walking vertebrates, would be apparent as discontinuities in the experimental phase relationships; none are obvious, however, indicating continuous transitions between ICPs.

Discussion

A large body of data shows that walking at high speeds is associated with tripod coordination in insects, while tetrapod-like and wave gait-like coordination patterns are more frequent at lower speeds. The present work questions why insects change their interleg coordination during walking in such a speed-dependent manner. To address this, we created a static stability-based model (Fig. 2) for predicting ICPs during walking in six-legged insects. The model takes into account basic kinematic parameters (Fig. 1 and Fig. 2C) found in walking fruit flies and explicitly accommodates walking speed as an important aspect. Using this model, we exhaustively explored ipsilateral and contralateral interleg phase relationships over the complete range of walking speeds and analyzed the influence of these phases on static stability (Fig. 5), as well as how tolerant to error these phases are before the animal is no longer statically stable (Fig. 6). Furthermore, we compared the predicted optimal phase relationships to a large body of experimental data measured in the present as well as a previous study (Wosnitza et al., 2013). The results suggest that static stability plays an important role in the selection of an ICP at a particular speed. The model predicts several experimentally observed aspects of insect walking. First, ICPs form a continuum spanning the complete range of walking speeds. Furthermore, it predicts constant contralateral phase relationships of 0.5 and a speed-dependence of ipsilateral phase relationships; this is in line with the experimental data presented here that suggest that idealized tetrapod coordination is in fact not utilized by walking flies (Fig. 8). The model also provides a potential explanation for the experimentally observed reduction in phase variability at high walking speeds, namely the reduced range of phase values that provide non-zero static stability (Fig. 5). Finally, an anteriorly directed progression of swing phases in ipsilateral legs emerges in the model (Fig. 7). This is a general invariant feature of insect walking and is readily explained by the model.

ICPs change continuously with walking speed

The model predicts an animal's preferred ICP at each speed, assuming that animals choose the ICP that balances static stability and robustness. Furthermore, the speed-invariant contralateral phase angle is predicted to be 0.5, which is also observed in experimental data. The model's prediction of the ipsilateral phase angle represents one boundary in the experimental data and a sharp edge of static stability for the model. This suggests that the animal does not use the most stable ICP, but instead prefers slightly less stable, but more robust ICP at a given speed. Regardless, the animal does prefer ICPs that are more stable than tripod at every speed, with no discontinuous jump to tripod at high speeds. Even if de-affarented insect ganglia can produce tripod-like output (Fuchs et al., 2011), we argue that such functionality is of lesser importance for the intact, behaving animal. Of course, the purely behavioral level addressed in our study cannot settle this question conclusively. Instead, it is likely that a combination of central neural mechanisms and mechanical influences contribute to the animal's variable, adaptive locomotion.

Our model predicts continuous transitions between ICPs as the walking speed changes, suggesting that fruit flies, and by extension other insects, may not exhibit true gaits like those observed in vertebrates; gait transitions would manifest as discontinuities in such a speed-dependent analysis. Indeed, the experimental data that we collected also showed no evidence of discontinuities indicative of gait transitions. This is an important distinction to make, because the control of a continuous transition of ICPs may be very different from that for discontinuous gait transitions. While many mechanisms underlying vertebrate and invertebrate locomotion are similar due to convergent evolution (Ritzmann et al., 2004), the control of interleg coordination may be one mechanism that is fundamentally different between these groups. Such a difference could drive a search for structural and functional differences between the processing of interleg signals in spinal cords and ventral nerve cords. In addition, understanding why these groups may have evolved different strategies may inform the design of legged robot control systems; for example, there may be energetic or control effort advantages for small robots to use a continuum of ICPs while large robots use discontinuous gaits.

We believe that the data presented in this work, and data from previous studies in *Drosophila* (Berendes et al., 2016; Wosnitza et al., 2013), support abandoning the term *gait* when referring to insect ICPs, because insect interleg coordination does not fall into discrete coordination patterns. Instead, insect ICPs may be thought of as a continuum of stance durations (Dürr et al., 2018). Based on these findings, we would like to emphasize that

walking speed has a strong influence on the parameters measured here (phase relationships and footfall patterns), supporting the results from Graham (1972). Studies investigating walking in insects should, therefore, explicitly take into account and measure walking speed to avoid conflating true changes in walking parameters between experimental conditions with mere changes in walking speed.

Idealized tetrapod ICPs are not preferred

Both our model and the data we collected suggest that *D. melanogaster* does not utilize the idealized tetrapod ICP, in which three pairs of legs sequentially enter swing phase together. While our model suggests that the idealized tetrapod with (ϕ_C, ϕ_I) = (1/3, 1/3) should be a stable ICP (see Fig. 4B and C, as well as Fig. 5), it would be less robust than the observed ICP where (ϕ_C, ϕ_I) = (1/2, 1/3). This is because small changes to either ϕ_I or ϕ_C from (ϕ_C, ϕ_I) = (1/3, 1/3) would destabilize the animal, whereas ϕ_C would have to change substantially from (ϕ_C, ϕ_I) = (1/2, 1/3) to destabilize the animal. Previous studies of walking in *D. melanogaster* have also reported that contralateral legs remain in antiphase at all walking speeds, never giving rise to the idealized tetrapod gait (Strauss and Heisenberg, 1990). Keeping contralateral legs in antiphase at all speeds is also consistent with behavioral descriptions of arthropod interleg coordination (Cruse, 1990b) and could potentially simplify interleg control.

Insect interleg coordination is likely determined by more than just the static stability over the course of one step cycle, because the model's static stability predicted more extreme speed-dependent changes in ICP (Fig. 5). This discrepancy might be explained by considering the robustness of the coordination pattern—that is, how much error in the interleg phasing can be tolerated before destabilizing the body. By this measure, our model would predict that the animal uses tripod coordination at all speeds (Fig. 6). Taking robustness into consideration, the data suggest that the animal instead utilizes a compromise between the most stable and most robust ICP at a given walking speed, showing variation in the ICP but avoiding potentially unstable ICPs. In fact, the mean (ϕ_I, ϕ_C) of the animal data always lies near the 80th percentile of stable ICPs (data not shown). This means that 20% of other available ICPs would be more stable. In our comparison between model and experimental data (Fig. 7), the predicted most stable ipsilateral phases (magenta line) seem to constitute a lower bound for the experimental data, and the experimental data's average is always between the most stable and most robust phases; this observation is compatible with the hypothesis that the motor output reflects the expected variability.

Extensions of the model

Although our model successfully captured the experimental data collected for this study, there are different locomotion scenarios that could be used to test this model in the future. These fall into two main categories: support polygon variant and gravity vector variant. Support polygon variant scenarios include animals with amputated legs and walking along a curved path. In this study, we restricted analysis to intact animals, walking along paths with a very low curvature. However, removing legs drastically affects the support polygon and leads to noticeable changes in ICP in both fruit flies (Wosnitza et al., 2013) and cockroaches (Delcomyn, 1971; Hughes, 1957). In addition, the stance trajectories of fruit fly walking along a curved path are markedly different than during straight walking (Szczecinski et al., 2018). Changing the stance trajectories of each foot also changes the associated support polygon and, as a consequence, static stability.

Gravity vector variant scenarios include animals walking on inclined, vertical, or inverted substrates. In such cases, the animal is not trying to prevent falling directly toward the substrate as in level locomotion, but at some angle to it, along it, or away from it, respectively. Maintaining stability in such cases would benefit from or require adhesive forces between the animal's foot and the substrate. In fact, larger insects, such as stick insects, appear to use such mechanisms to improve stability even when walking on flat substrates (Gorb, 1998; Paskarbeit et al., 2016). Studies of insect-inspired climbing robots have shown that the stability of climbing can be analyzed in a very similar way to how we analyzed the static stability of walking here, but with the addition of a force tangential to the substrate, provided by the "uphill" leg (Daltorio et al., 2009). In the future, we will expand our model and test its ability to predict ICPs of climbing fruit flies.

Possible mechanisms in the animal

The goal of this work was not to explain how the animal generates different ICPs, but why. However, it is worth considering what mechanisms may give rise to the phenomena measured in this work. Behavioral rules that describe interleg coordination in arthropods have long been known (Cruse, 1990a; Dallmann et al., 2017; Dürr et al., 2004). Several of these behavioral rules explicitly address the temporal coordination between onsets of the swing phases in adjacent legs (Rules 1-3, see Dürr et al., 2004). As a consequence, they ensure that the probability of two adjacent legs executing their swing movements simultaneously is low. Recent work with stick insects has shown that the onset of swing phase in a middle leg correlates very tightly with the onset of stance phase in the ipsilateral hind leg (Dallmann et al., 2017). The authors suggest that this is due to the middle leg measuring a decrease in the load being supported, causing the leg to enter swing phase.

Indeed, campaniform sensilla, which sense cuticular strain induced by load changes, have been found to be sensitive to unloading in the cockroach (Zill et al., 2009). Such a mechanism could be seen as an indirect measurement of the animal's stability affecting their ICP. Whether this plays a role in *D. melanogaster*, a particularly light animal, in which gravitational forces might not play a very large role, remains to be investigated.

Interestingly, the previously mentioned interleg coordination rules (Dürr et al., 2004) strongly favor an anteriorly directed swing phase progression (AD SPP), which is also strongly favored by our static stability-based model (Fig. 7). Based on our results, this phenomenon can be generally explained in such a way that the spatial relationship between a middle leg and its ipsilateral front and hind legs strongly affects static stability during the time of lift off of either of the latter legs. During AD SPP, support is handed off smoothly from either the front or hind leg to the middle leg, because the current position of the middle leg is close to the now lifted-off leg. This concept can probably be generalized to all six-legged animals, since it should be independent of the exact morphology or position of the COM. Moreover, a switch to backward walking would result in a posteriorly directed SPP. Interestingly, evidence for this can be found in backward walking fruit flies (Bidaye et al., 2014) and stick insects (Jeck and Cruse, 2007), in which the SPP is reversed.

There is also evidence that walking in insects is more determined by centrally generated motor output at high walking speeds, while the influence of leg sensory structures is reduced (Bender et al., 2011; Cruse et al., 2007). This is further supported by recent studies *C. morosus* (Mantziaris et al., 2017), *C. gregaria* (Knebel et al., 2017), and *D. melanogaster* (Berendes et al., 2016). These studies have shown that neighboring legs have preferred phases of oscillation, even when local sensory feedback is absent. This reduced sensory influence at high walking speeds could, in turn, make the motor output less variable, thus facilitating the convergence to the narrow range of stable ICPs. Ultimately, interleg coordination likely arises through a combination of mechanisms that are mediated both mechanically and neurally. On a more general note, the fact that similar phenomena can be observed in a holometabolous insect (here: *D. melanogaster*) as well as in a hemimetabolous insect (e.g., *C. morosus*) might suggest that the principles explored here are representative for walking insects, in general.

Does the animal acutely measure static stability?

Assuming that static stability plays a role for the speed-dependent selection of ICP, an important question is whether static stability, or some related proxy, is measured acutely and continuously during walking or if the evolutionary pressure to remain upright resulted in interleg coordination rules that keep the body upright. Our experimental data from tethered

animals whose bodies were supported during walking did not noticeably vary from those from freely walking individuals. In principle, these animals cannot fall over and acute measurement of stability would result in different ICPs. These observations, which are consistent with comparable experiments in other animals such as the stick insect *C. morosus*, suggest that walking flies do not measure stability as directly as mammals do, for example, by utilizing vestibular input (Buschmann et al., 2015).

The consequences of falling are less severe for a fruit fly than for larger animals (Hooper, 2012); if they do misstep and fail to support their body, their large damping to mass ratio should slow down their fall more than for larger animals, such as humans. Nevertheless, fruit flies still need to stay upright during walking. Falling impedes the animal's progress and wastes energy and time, suggesting that it would benefit the animal to remain upright. This might be even more critical during behaviors like courtship, during which males chase females in close pursuit (Hall, 1994); falling over in this situation might reduce the chances of mating. A similar line of argument can be made for escape from predators, in which precise and smooth stepping is required (Parigi et al., 2014). Stability and the need to remain upright have likely influenced the evolution of the observed ICPs in insects.

List of symbols and abbreviations

ϕ_I: Ipsilateral phase relationship

ϕ_I: Contralateral phase relationship

AD: Anteriorly directed

AEP: Anterior extreme position

BL: Body length

COM: Center of mass

ICP: Interleg coordination pattern

IR: Infrared

LED: Light-emitting diode

PD: Posteriorly directed

PEP: Posterior extreme position

PP: Polypropylene

SPP: Swing phase progression

w^{1118}: *D. melanogaster white* mutant strain

WT: *D. melanogaster* wildtype strains *Berlin* and *CantonS*

Acknowledgements

The authors would like to thank Michael Dübbert and Jan Sydow for excellent technical support, Corinna Rosch for animal husbandry, and Sima Seyed-Nejadi, Sherylane Seeliger, and Hans-Peter Bollhagen for lab support.

Competing interests

The authors declare no competing or financial interests.

Author contributions

N.S.S., T.B., and A.B. conceived the study, N.S.S., T.B., and A.S.C. carried out the experiments, N.S.S. and T.B. created the model, N.S.S., T.B., and A.S.C. analyzed experimental data, N.S.S., T.B., A.S.C., and A.B. wrote the manuscript. All authors read and approved the final manuscript.

Funding

This study was supported by the German Research Foundation (DFG-Grant GRK 1960, Research Training Group *Neural Circuit Analysis*, to A.B.), the Graduate School for Biological Sciences at the University of Cologne (to A.S.C.), and the National Science Foundation (Grant 1704436, to N.S.S.).

References

Alexander, R. M. (1989). Optimization and gaits in the locomotion of vertebrates. *Physiol. Rev.* **69**, 1199–1227.

Ayali, A., Borgmann, A., Büschges, A., Couzin-Fuchs, E., Daun-Gruhn, S. and Holmes, P. (2015). The comparative investigation of the stick insect and cockroach models in the study of insect locomotion. *Curr. Opin. Insect Sci.* **12**, 1–10.

Backhaus, B., Sulkowski, E. and Schlote, F. (1984). A semi-synthetic, general-purpose medium for Drosophila melanogaster. *Dros Inf Serv* **60**, 210–212.

Bender, J. A., Simpson, E. M., Tietz, B. R., Daltorio, K. A., Quinn, R. D. and Ritzmann, R. E. (2011). Kinematic and behavioral evidence for a distinction between trotting and ambling gaits in the cockroach Blaberus discoidalis. *J. Exp. Biol.* **214**, 2057–2064.

Berendes, V., Zill, S. N., Büschges, A. and Bockemühl, T. (2016). Speed-dependent interplay between local pattern-generating activity and sensory signals during walking in Drosophila. *J. Exp. Biol.* jeb.146720.

Bidaye, S. S., Machacek, C., Wu, Y. and Dickson, B. J. (2014). Neuronal control of Drosophila walking direction. *Science* **344**, 97–101.

Bidaye, S. S., Bockemühl, T. and Büschges, A. (2017). Six-legged walking in insects: how CPGs, peripheral feedback, and descending signals generate coordinated and adaptive motor rhythms. *J. Neurophysiol.* **119**, 459–475.

Borgmann, A. and Büschges, A. (2015). Insect motor control: methodological advances, descending control and inter-leg coordination on the move. *Curr. Opin. Neurobiol.* **33**, 8–15.

Buschmann, T., Ewald, A., von Twickel, A. and Büschges, A. (2015). Controlling legs for locomotion - insights from robotics and neurobiology. *Bioinspir. Biomim.* **10**,.

Cruse, H. (1990b). What mechanisms coordinate leg movement in walking arthropods? *Trends Neurosci.* **13**, 15–21.

Cruse, H., Dürr, V. and Schmitz, J. (2007). Insect walking is based on a decentralized architecture revealing a simple and robust controller. *Philos. Trans. R. Soc. Math. Phys. Eng. Sci.* **365**, 221–250.

Dallmann, C. J., Hoinville, T., Du, V. and Schmitz, J. (2017). A load-based mechanism for inter-leg coordination in insects.

Daltorio, K. A., Wei, T. E., Horchler, A. D., Southard, L., Wile, G. D., Quinn, R. D., Gorb, S. N. and Ritzmann, R. E. (2009). Mini-Whegs TM Climbs Steep Surfaces Using Insect-inspired Attachment Mechanisms ,
Mini-Whegs TM Climbs Steep Surfaces Using Insect-inspired Attachment Mechanisms. *Int. J. Robot. Res.* **28**, 285–302.

Delcomyn, F. (1971). The Effect of Limb Amputation on Locomotion in the Cockroach Periplaneta Americana. *J ExpBiol* **54**, 453–469.

Dürr, V., Schmitz, J. and Cruse, H. (2004). Behaviour-based modelling of hexapod locomotion : linking biology and technical application. *Arthropod Struct. Dev.* **33**, 237–250.

Dürr, V., Theunissen, L. M., Dallmann, C. J., Hoinville, T. and Schmitz, J. (2018). Motor flexibility in insects: adaptive coordination of limbs in locomotion and near-range exploration. *Behav. Ecol. Sociobiol.* **72**,.

Fuchs, E., Holmes, P., Kiemel, T. and Ayali, A. (2011). Intersegmental coordination of cockroach locomotion: adaptive control of centrally coupled pattern generator circuits. *Front. Neural Circuits* **4**, 125.

Full, R. J. and Tu, M. S. (1990). Mechanics of six-legged runners. *J Exp Biol* **148**, 129–46.

Gorb, S. N. (1998). The design of the fly adhesive pad: distal tenent setae are adapted to the delivery of an adhesive secretion. *Proc. R. Soc. Lond. B Biol. Sci.* **265**, 747–752.

Gowda, S. B. M., Paranjpe, P. D., Reddy, O. V., Thiagarajan, D., Palliyil, S., Reichert, H. and VijayRaghavan, K. (2018). GABAergic inhibition of leg motoneurons is required for normal walking behavior in freely moving *Drosophila*. *Proc. Natl. Acad. Sci.* **115**, 201713869.

Graham, D. (1972). A behavioural analysis of the temporal organisation of walking movements in the 1st instar and adult stick insect (Carausius morosus). *J. Comp. Physiol.* **81**, 23–52.

Hall, J. C. (1994). The mating of a fly. *Science* **264**, 1702–1714.

Hooper, S. L. (2012). Body size and the neural control of movement. *Curr. Biol.* **22**, R318–R322.

Hooper, S. L., Guschlbauer, C., Blümel, M., Rosenbaum, P., Gruhn, M., Akay, T. and Büschges, A. (2009). Neural control of unloaded leg posture and of leg swing in stick insect, cockroach, and mouse differs from that in larger animals. *J. Neurosci. Off. J. Soc. Neurosci.* **29**, 4109–19.

Hoyt, D. F. and Taylor, C. R. (1981). Gait and the Energetics of Locomotion in Horses. *Nature* **292**, 239–240.

Hughes, G. M. (1952). The Co-Ordination of Insect Movements. I. The Walking Movements of Insects. *J. Exp. Biol.* **29**, 267–285.

Hughes, G. M. (1957). The Co-Ordination of Insect Movements: 11. The Effect of Limb Amputation and the Cutting of Commissures In The Cockroach (Blatta Oiuentalis). *J Exp Biol* **34**, 306–333.

Jeck, T. and Cruse, H. (2007). Walking in Aretaon asperrimus. *J. Insect Physiol.* **53**, 724–733.

Knebel, D., Ayali, A., Pflüger, H. J. and Rillich, J. (2017). Rigidity and Flexibility: The Central Basis of Inter-Leg Coordination in the Locust. *Front Neural Circuits* **10**, 112.

Mantziaris, C., Bockemühl, T., Holmes, P., Borgmann, A., Daun, S. and Büschges, A. (2017). Intra- and intersegmental influences among central pattern generating networks in the walking system of the stick insect. *J. Neurophysiol.* **49**, jn.00321.2017.

McGhee, R. B. and Frank, A. A. (1968). On the stability properties of quadruped creeping gaits. *Math. Biosci.* **3**, 331–351.

Mendes, C. S., Bartos, I., Akay, T., Márka, S. and Mann, R. S. (2013). Quantification of gait parameters in freely walking wild type and sensory deprived Drosophila melanogaster. *eLife* **2013**, 1–24.

Nishii, J. (2000). Legged insects select the optimal locomotor pattern based on the energetic cost. *Biol. Cybern.* **83**, 435–42.

Orlovsky, G. N., Deliagina, T. G. and Grillner, S. (1999). *Neuronal Control of Locomotion: From Mollusc to Man*. New York: Oxford University Press, USA.

Parigi, A., Porter, C., Cermak, M., Pitchers, W. R. and Dworkin, I. (2014). How predator hunting-modes affect prey behaviour: Capture deterrence in Drosophila melanogaster. *bioRxiv*.

Paskarbeit, J., Otto, M., Schilling, M. and Schneider, A. (2016). Stick(y) Insects — Evaluation of Static Stability for Bio-inspired Leg Coordination in Robotics. *Conf. Biomim. Biohybrid Syst.* **1**, 239–250.

Ramdya, P., Thandiackal, R., Cherney, R., Asselborn, T., Benton, R., Ijspeert, A. J. and Floreano, D. (2017). Climbing favours the tripod gait over alternative faster insect gaits. *Nat. Commun.* **8**, 1–11.

Ritzmann, R. E., Quinn, R. D. and Fischer, M. S. (2004). Convergent evolution and locomotion through complex terrain by insects, vertebrates and robots. *Arthropod Struct. Dev.* **33**, 361–379.

Schilling, M., Hoinville, T., Schmitz, J. and Cruse, H. (2013). Walknet, a bio-inspired controller for hexapod walking. *Biol. Cybern.* **107**, 397–419.

Seelig, J. D., Chiappe, M. E., Lott, G. K., Dutta, A., Osborne, J. E., Reiser, M. B. and Jayaraman, V. (2010). Two-photon calcium imaging from head-fixed Drosophila during optomotor walking behavior. *Nat. Methods* **7**, 535–40.

Simon, J. C. and Dickinson, M. H. (2010). A New Chamber for Studying the Behavior of Drosophila. *PLOS ONE* **5**, e8793.

Smolka, J., Byrne, M. J., Scholtz, C. H. and Dacke, M. (2013). A new galloping gait in an insect. *Curr. Biol.* **23**, R913–R915.

Spirito, C. P. and Mushrush, D. L. (1979). Interlimb Coordination During Slow Walking in the Cockroach: I. Effects of Substrate Alterations. *J. Exp. Biol.* **78**, 233–243.

Strauss, R. and Heisenberg, M. (1990). Coordination of legs during straight walking and turning in Drosophila melanogaster. *J. Comp. Physiol. A Neuroethol. Sens. Neural. Behav. Physiol.* **167**, 403–12.

Szczecinski, N. S., Büschges, A. and Bockemühl, T. (2018). Direction-Specific Footpaths Can Be Predicted by the Motion of a Single Point on the Body of the Fruit Fly Drosophila Melanogaster. In *Conference on Biomimetic and Biohybrid Systems*, pp. 477–489.

Turns, S. R. (2006). *Thermal-Fluid Sciences : an Integrated Approach*. Cambridge University Press.

Wahl, V., Pfeffer, S. E. and Wittlinger, M. (2015). Walking and running in the desert ant Cataglyphis fortis. *J Comp Physiol Neuroethol Sens Neural Behav Physiol* **201**, 645–56.

Wendler, G. (1964). Laufen und Stehen der Stabheuschrecke Carausius morosus: Sinnesborstenfelder in den Beingelenken als Glieder von Regelkreisen. *Z. Für Vgl. Physiol.* **48**, 198–250.

Wilshin, S., Reeve, M. A., Haynes, G. C., Revzen, S., Koditschek, D. E. and Spence, A. J. (2017). Longitudinal quasi-static stability predicts changes in dog gait on rough terrain. *J. Exp. Biol.* **220,** 1864–1874

Wilson, D. M. (1966). Insect walking. *Annu. Rev. Entomol.* **11**, 103–122.

Wosnitza, A., Bockemühl, T., Dübbert, M., Scholz, H. and Büschges, A. (2013). Inter-leg coordination in the control of walking speed in Drosophila. *J. Exp. Biol.* **216**, 480–491.

Zill, S. N., Keller, B. R. and Duke, E. R. (2009). Sensory Signals of Unloading in One Leg Follow Stance Onset in Another Leg: Transfer of Load and Emergent Coordination in Cockroach Walking. *J. Neurophysiol.* **101**, 2297–2304.

Figures

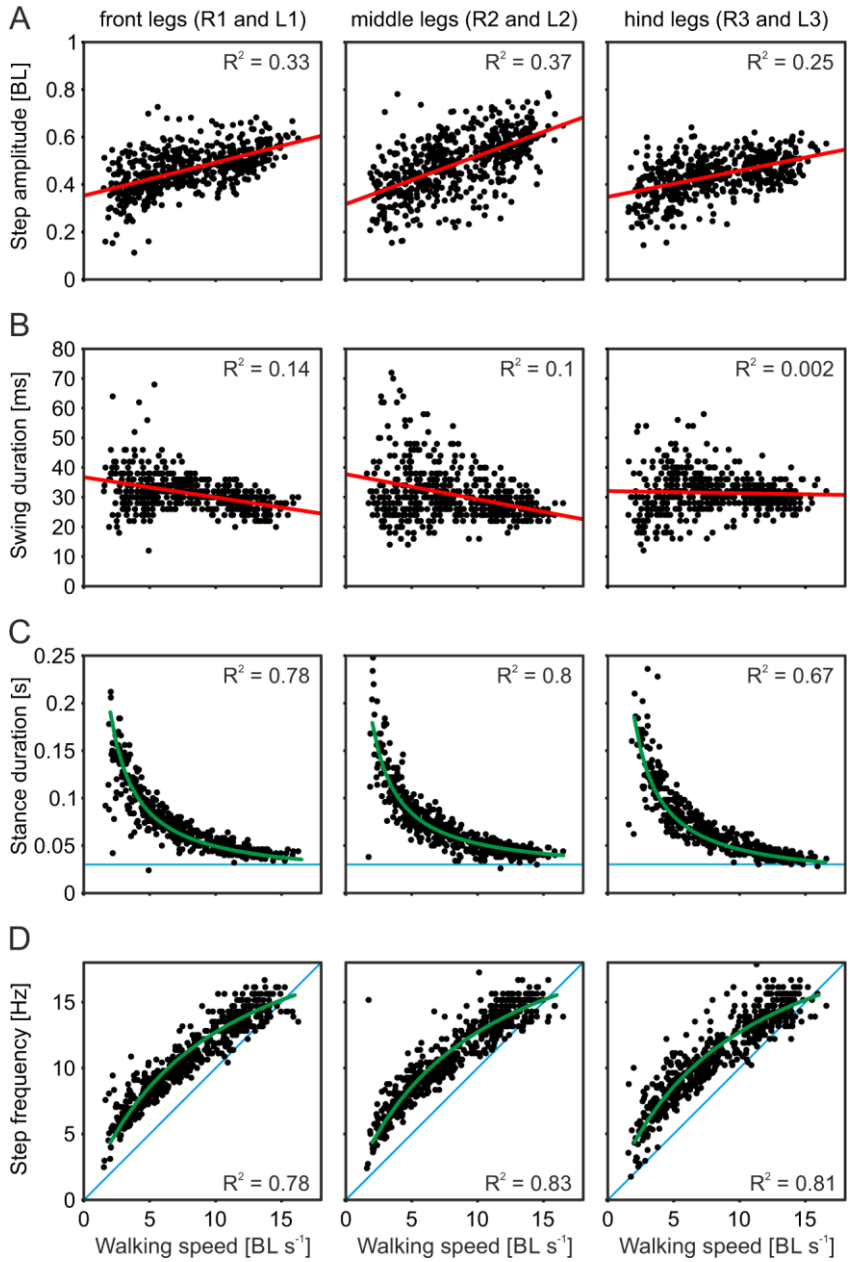

Figure 1: Basic parameters of walking *D. melanogaster* expressed as a function of walking speed. Points correspond to individual steps. Left column corresponds to front legs (left and right, L1 and R1), middle column to middle legs (L2 and R2), right column to hind legs (L3 and R3). (A) Step amplitude is only weakly correlated with walking speed (regression line in red). (B) Swing duration is constant over the observed speed range (regression line in red).

(C and D) Stance duration and step frequency are strongly correlated with walking speed; both can be predicted with high accuracy (green lines and corresponding coefficients of determination in C and D). For comparison, blue lines in C indicate swing duration, in D they indicate a linear relationship between speed and frequency. This figure was created with experimental data from Wosnitza et al. (2013).

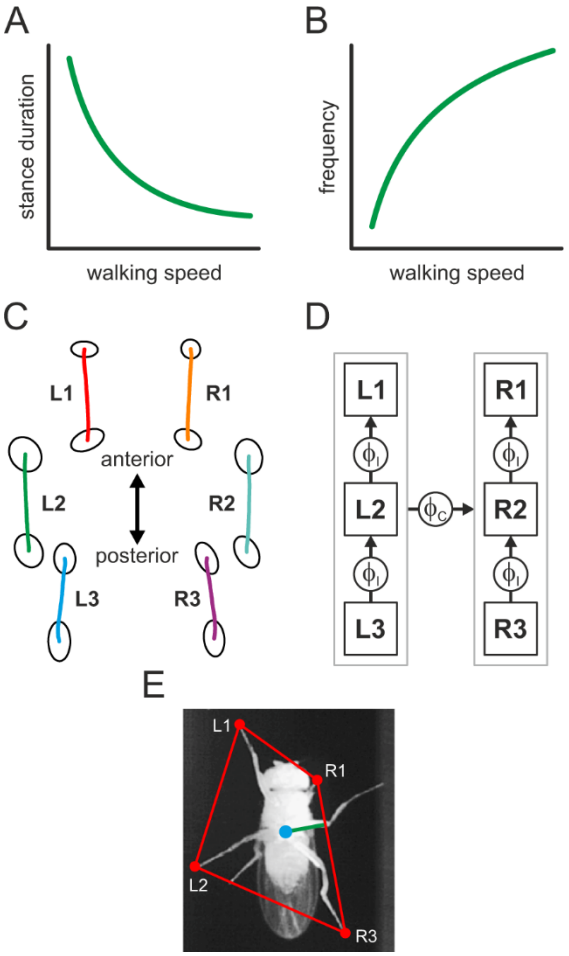

Figure 2: Kinematic model and static stability. (A and B) Walking speed predicts stance duration and stepping frequency (see also Fig. 1C and D), resulting in a temporal sequence of swing and stance movements for each leg. (C) Average stance trajectories from experiments are combined with this temporal sequence. AEPs, PEPs, and stance trajectories are described in body-centered coordinates. Ellipses around AEPs and PEPs indicate one standard deviation of experimental positional variability (however, only the average stance trajectories were used here). (D) ϕ_I and ϕ_C, describe the phase relationships between ipsilateral legs and contralateral body sides, respectively (arrows point from reference leg to analyzed leg). (E) For a given set of ϕ_I and ϕ_C and a particular time within the step cycle, it can be determined which legs are in stance and what their positions are with regard to the COM (blue dot). The legs currently in stance form a convex hull (red); the minimal distance between the COM and the convex hull defines static stability (green line) for this posture.

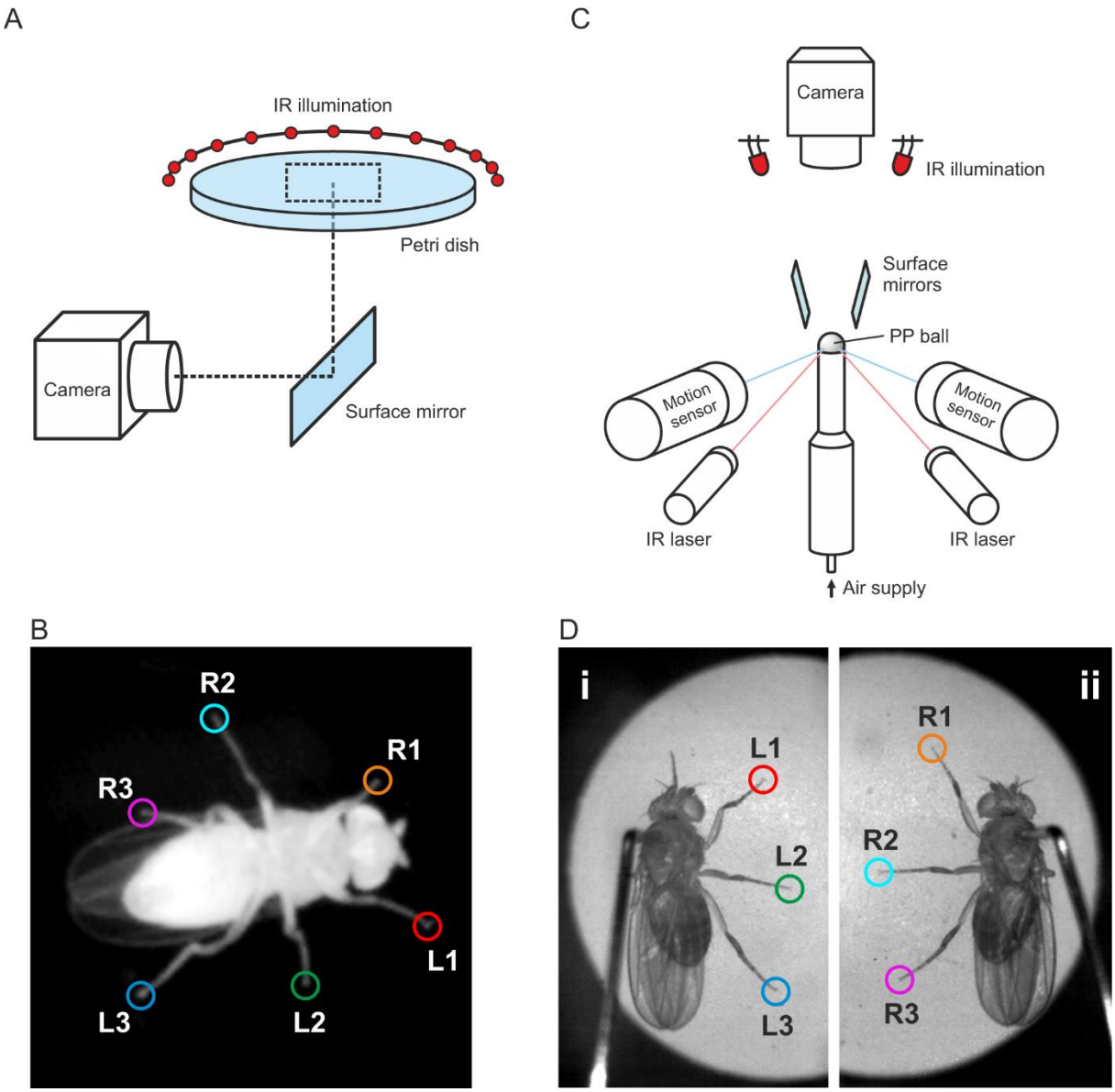

Figure 3: Experimental setups. (A) Free-walking setup. Flies walked on top of a glass petri dish covered with a watch glass (not shown for clarity). A concentric ring of IR LEDs provided illumination (ring only shown partially). A high-speed camera captured a rectangular area of the petri dish (dashed rectangle) via a surface mirror. (B) Example from a video frame captured in the free-walking setup. Leg tips were manually annotated (for labels see Fig. 1). (C) Tethered-walking setup. Flies walked on an air-supported PP ball whose rotational movements were captured by two motion sensors. Illumination for the sensors was provided by IR lasers. The top of the ball and two mirrors were captured with a high-speed camera; illumination was provided by an LED ring around the camera lens. (D) Two surface mirrors provided side views of the fly (leg tips annotated manually).

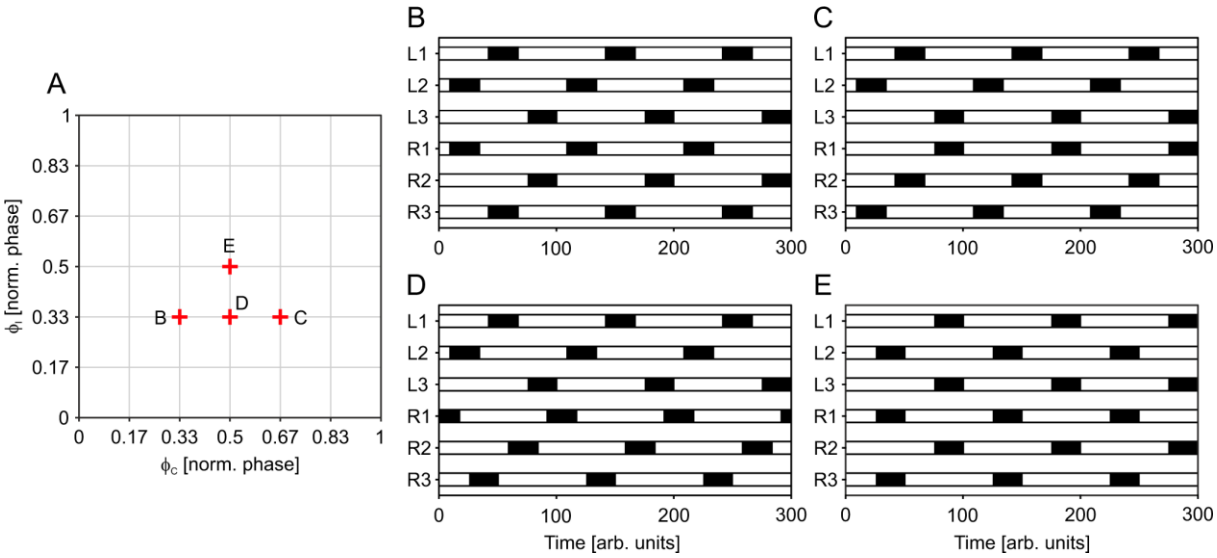

Figure 4: Hypothetical inter-leg coordination patterns (ICPs). Each combination of ϕ_I and ϕ_C in the model (see Fig. 2) is associated with a particular ICP. (A) ϕvϕ plot with the position of four exemplary ICPs; each indicated point (B, C, D, E) corresponds to an ICP in panels B to E. (B and C) Idealized tetrapod ICPs commonly referred to in the literature. These correspond to ϕ_I = 1/3 and ϕ_C = 1/3 or 2/3. (D) Tetrapod-like ICP for which ϕ_I = 1/3 and ϕ_C = 1/2. This pattern can be found in walking fruit flies and is also predicted as more stable than the ideal tetrapod ICP (see Results). (E) Tripod ICP corresponding to ϕ_I = 1/2 and ϕ_C = 1/2. This ICP has frequently been reported in the literature. For comparison, walking speed for all exemplary ICPs has been set to 5 BL s^{-1}.

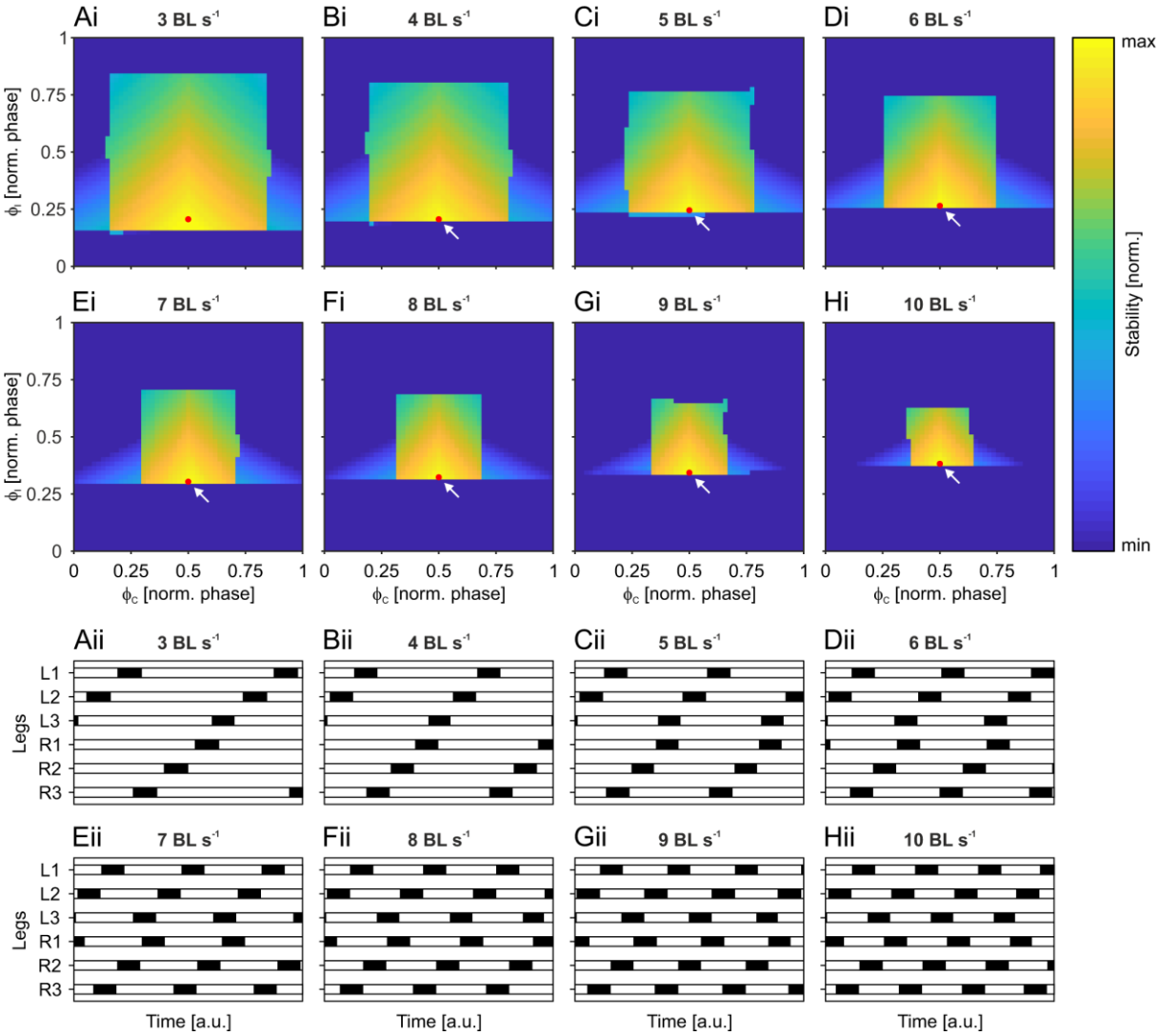

Figure 5: Model-derived static stability and corresponding ICPs. (Ai to Hi) Each combination of ϕ_I and ϕ_C is associated with a particular stability at a particular walking speed (here 3 to 10 BL s^{-1}). High static stability is indicated by yellow hues, low or zero stability by blue hues. In each $\phi v \phi$ plot, the point of maximum stability is indicated (red dot). Points of maximum stability are very close to regions of zero stability (white arrows). (Aii to Hii) ICPs that correspond to ϕ_I and ϕ_C of maximum stability in Ai to Hi. ICPs continuously change from wave gait-like coordination at low speeds to almost tripod coordination at high speeds.

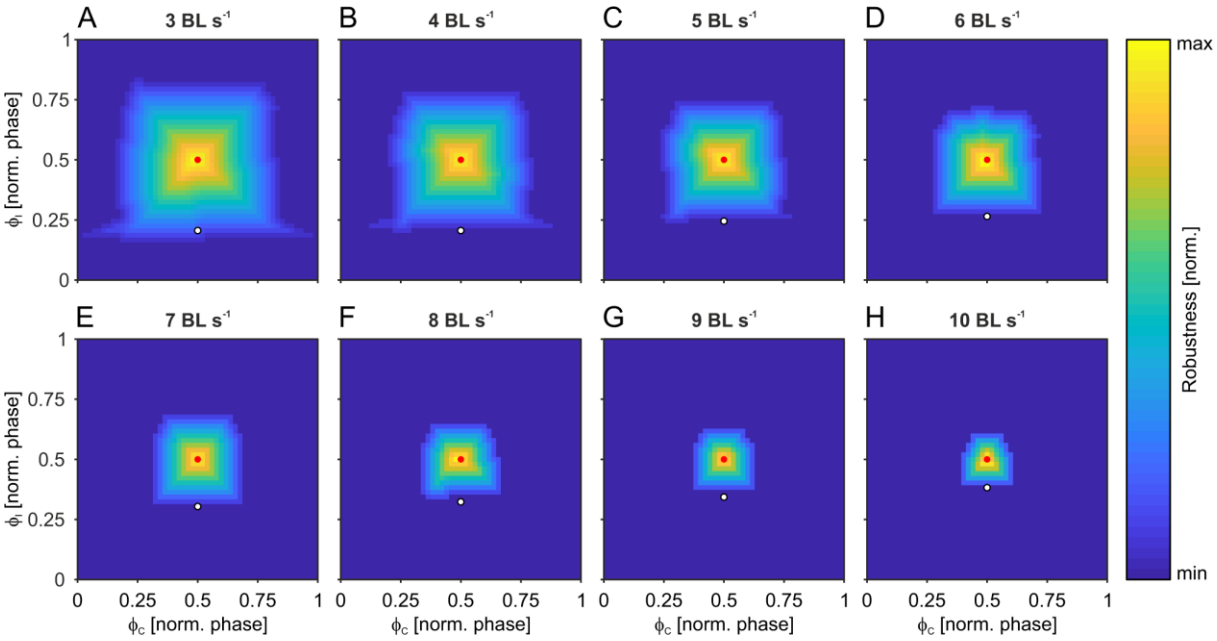

Figure 6: Model-derived robustness. (A to H) Each combination of ϕ_I and ϕ_C is associated with a particular robustness at a particular walking speed (here 3 to 10 BL s^{-1}, see also Fig. 5Ai to Hi). High robustness is indicated by yellow hues, low or zero robustness by blue hues. In contrast to static stability, the phase relationships associated with the highest robustness are always identical or close to ϕ_I = 1/2 and ϕ_C = 1/2 (red dots). For comparison, combinations of ϕ_I and ϕ_C with highest static stability are indicated by white dots (also see Fig. 5Ai-Hi).

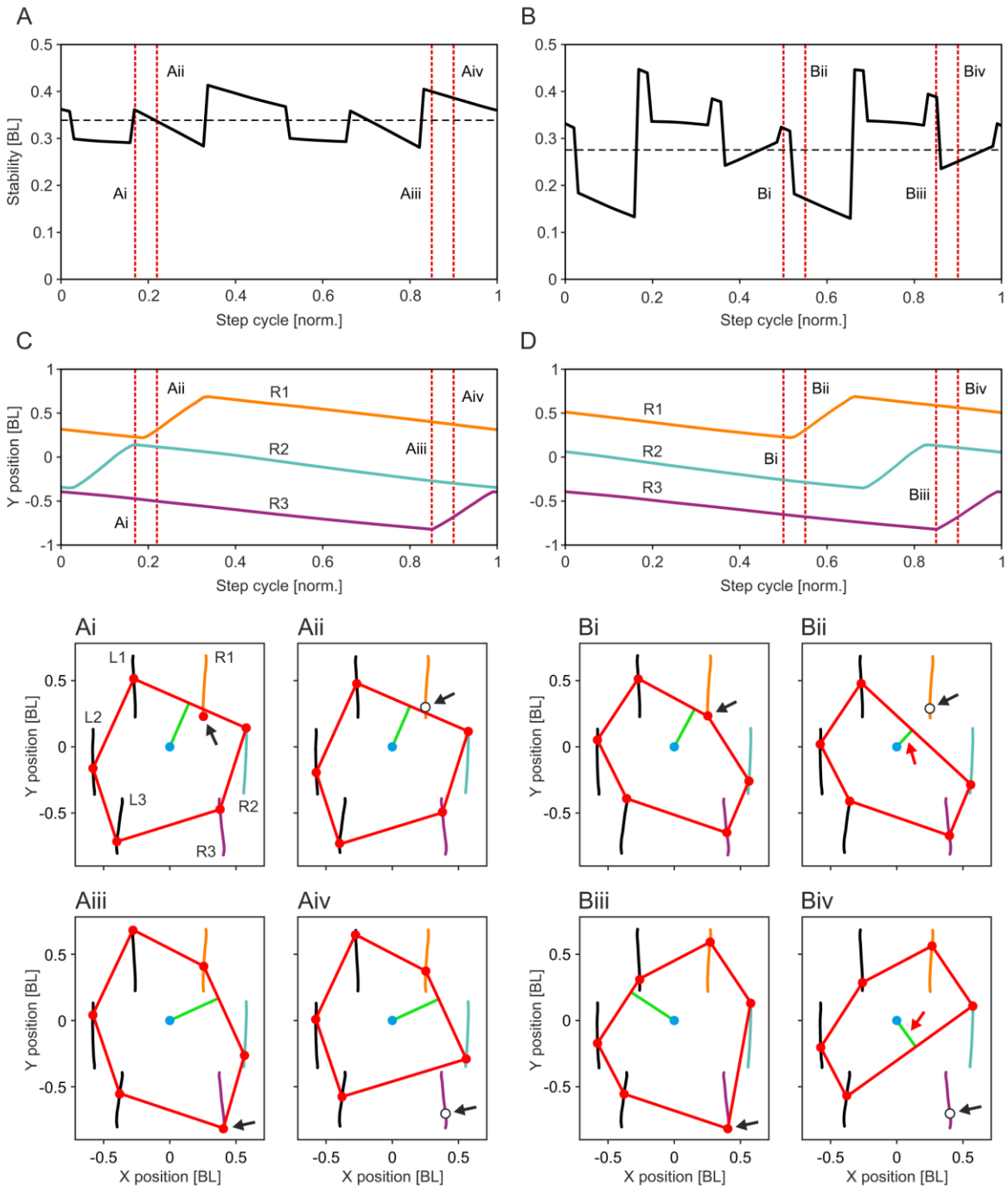

Figure 7: Anteriorly directed swing phase progression (AD SPP) is more stable. (A and B) Static stability over one normalized step cycle during AD SPP (A, ϕ_I is set to 1/6) and during posteriorly directed (PD) SPP (B, ϕ_I is set to 5/6). Average static stability is indicated by black dashed lines. Time points (Ai to Biv) of interest are indicated by red dashed lines (see corresponding panels). (C and D) Fore-aft position of right front (orange), middle (cyan), and hind (magenta) legs throughout one step cycle (see also A and B). (Ai and Aii) Stability polygons (red lines) during AD SPP around the time of lift-off of front leg R1 (Ai, shortly before; Aii, shortly after). (Aiii and Aiv) Stability polygons (red lines) during AD SPP around the time of lift-off of hind leg R3 (Aiii, shortly before; Aiv, shortly after). Panels Bi to Biv

correspond to the same time points during PD SPP. Black lines: stance trajectories, blue: COM, green: vector indicating static stability (see also Fig. 2E), red dots: touched-down leg, white dots: lifted-off legs, arrows highlight transitioning legs.

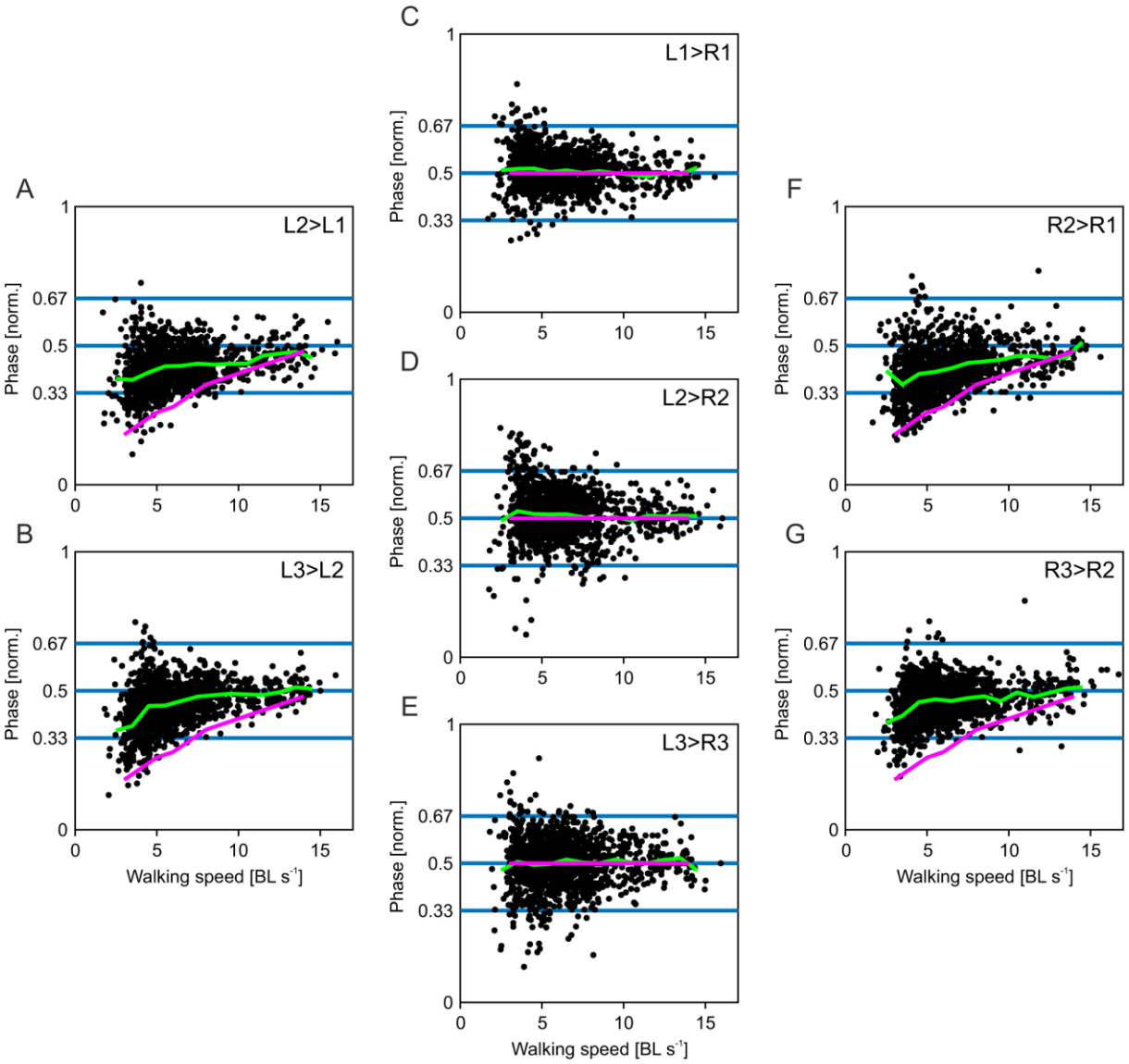

Figure 8: Phase relationships measured during experiments and predicted phases as a function of walking speed (new data and data from Wosnitza et al., 2013). Dots correspond to the phase relationship of individual steps (total number of steps: 9,552), and phase is measured between an observed leg and a reference leg (e.g., L3>L2 refers to the reference leg L3 and the observed leg L2, total number of contralateral comparisons: n = 4,372, ipsilateral: n = 5,849). (A, B, F, G) Phase relationships between ipsilateral middle and front legs (A and F) and hind legs and middle legs (B and G). (C, D, E) Phase relationships between contralateral front legs (C), middle legs (D), and hind legs (E). Green lines indicate running averages of experimentally measured phases; magenta lines indicate model predictions for stability-optimal values of ϕ_I (A, B, F, G) and ϕ_C (C, D, E).

	Fluid density, kg/m^3	Relative fluid velocity, $m\ s^{-1}$	Length scale, m	Dynamic viscosity, Ns/m^2	Re, unitless
Human/air	1.225	1	1	18E-6	≈ 68E3
Fly/air	1.225	30E-3	2E-3	18E-6	≈ 4
Human/honey	1450	30E-3	1	14	≈ 3

Table S1: Reynolds numbers of different animals walking through different fluids. The viscosity of air to a fly walking at 30 mm s^{-1} is like the viscosity of honey to a human walking at the same speed. In such a scenario, a person would not be able to make ballistic motions due to the damping from the viscous honey. By the same logic, walking in fruit flies is hardly a dynamic motion; instead, it is dominated by viscous forces from the air and elastic forces from its muscles.

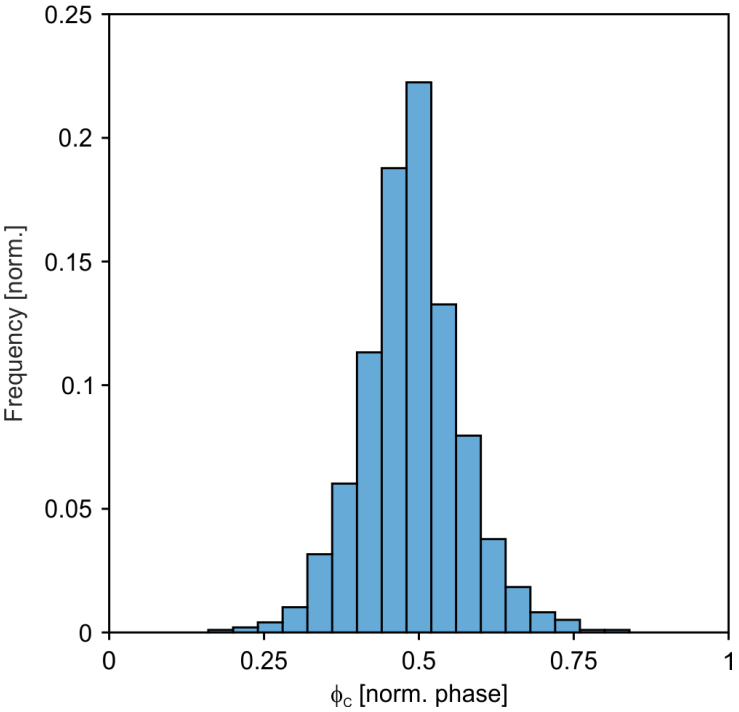

Figure S1: Distribution of contralateral phase relationships ϕ_C at walking speeds below 5 BL s^{-1}. Instead of a bimodal distribution, whose peaks would be centered at around 1/3 and 2/3, contralateral phases at low and intermediate walking speeds cluster around 0.5. This indicates anti-phasic stepping in contralateral legs of the same segment. Idealized tetrapod coordination (ϕ_C = 1/3 or 2/3) is observed rarely.